ResearchGate

See discussions, stats, and author profiles for this publication at: https://www.researchgate.net/publication/222565836

The time scale of the catalytic loop motion in triosephosphate isomerase

ARTICLE *in* JOURNAL OF MOLECULAR BIOLOGY · JULY 2001

Impact Factor: 4.33 · DOI: 10.1006/jmbi.2001.4672 · Source: PubMed

CITATIONS
101

READS
22

2 AUTHORS, INCLUDING:

Ann Mcdermott
Columbia University
100 PUBLICATIONS **4,019** CITATIONS

SEE PROFILE

Available from: Ann Mcdermott
Retrieved on: 24 January 2016

doi:10.1006/jmbi.2001.4672 available online at http://www.idealibrary.com on IDEAL® J. Mol. Biol. (2001) 310, 259–270

JMB

The Time scale of the Catalytic Loop Motion in Triosephosphate Isomerase

Sharon Rozovsky and Ann E. McDermott*

Department of Chemistry Columbia University, New York, NY 10027, USA

Loop 6 in the active site of Triosephosphate Isomerase (*Saccharomyces cerevisiae*) moves in order to reposition key residues for catalysis. The timescale of the opening and closing of this loop has been measured, at temperatures from −15 to +45 °C, using broadline solid state deuterium NMR of a single deuterated tryptophan located in the loop's N terminal hinge. The rate of the loop opening and closing was best detected using samples containing subsaturating amounts of a substrate analogue DL-glycerol 3-phosphate so that the populations of the open and closed forms were roughly equal, and using temperatures optimal for enzymatic function (30-45 °C). The T_2 values were much shorter than for unligated samples, consistent with full opening and closing of the loop at a rate of order 10^4 s^{-1}, and in good agreement with the rates estimated based on solution state ^{19}F NMR. The loop motion appears to be partially rate limiting for chemistry in both directions.

© 2001 Academic Press

Keywords: triosephosphate isomerase; protein dynamics; flexible loop; enzymatic catalysis; solid state NMR

*Corresponding author

Introduction

The catalytic reaction of triosephosphate isomerase (TIM) was one of the first clear demonstrations of the role of protein dynamics in promoting and controlling chemical reactivity. TIM catalyses the reversible isomerization of dihydroxyacetone phosphate (DHAP) to D-glyceraldehyde 3-phosphate (GAP), while suppressing elimination of orthophosphate (Richard, 1991; Rose, 1962). TIM is highly efficient in the thermodynamically "downhill" direction, with a k_{cat} value of 9×10^3 s^{-1}; enhancing the reaction by ten orders of magnitude over the reaction carried out under optimized solution conditions. TIM has therefore been described as an optimally efficient enzyme, or even as an exemplar of diffusion controlled reactivity. A vast body of kinetic, mechanistic and structural studies (Albery & Knowles, 1976a,b; Davenport *et al.*, 1991; Knowles, 1991; Komives *et al.*, 1991, 1995; Lodi & Knowles, 1991; Lolis *et al.*, 1990; Lolis & Petsko, 1990; Wierenga *et al.*, 1991) support a proton transfer-based mechanism involving a *cis*-enediol or enediolate intermediate (Rieder & Rose, 1959; Rose, 1962) (Figure 1(a)). The free-energy profile for the reaction was deduced from a series of deuterium and tritium isotope exchange experiments between the enzyme-substrate complex and the solvent (Albery & Knowles, 1976b). The rate-limiting step, in the thermodynamically unfavorable but metabolically crucial direction from DHAP to GAP, is not the proton transfer step, nor the diffusion of substrate to the enzyme, but is the loss of GAP product from the enzyme or, as Albery & Knowles (1976b) proposed, a slow conformational change preceding such a loss (Maister *et al.*, 1976). The relation between the proposed rate-limiting conformational change and the residence time of the intermediate or substrate suggests a role for conformational dynamics in coordination of the reaction (Alber *et al.*, 1983). Our aim is to characterize these conformational dynamics, and understand the relation between rate and enzyme optimization.

Loop 6, which contacts the active site, appears to move substantially during function (Figure 1(b)) (Alber *et al.*, 1981a; Joseph *et al.*, 1990; Lolis & Petsko, 1990; Phillips *et al.*, 1976). The loop has two conformers, an open and a closed state, the mechanistic purposes of which appear to be clear: the open conformation

Abbreviations used: TIM, triosephosphate isomerase; DHAP, dihydroxyacetone phosphate; GAP, D-glyceraldehyde 3-phosphate; G3P, DL-glycerol 3-phosphate.

E-mail address of the corresponding author: aem5@columbia.edu

0022-2836/01/010259–12 $35.00/0

© 2001 Academic Press

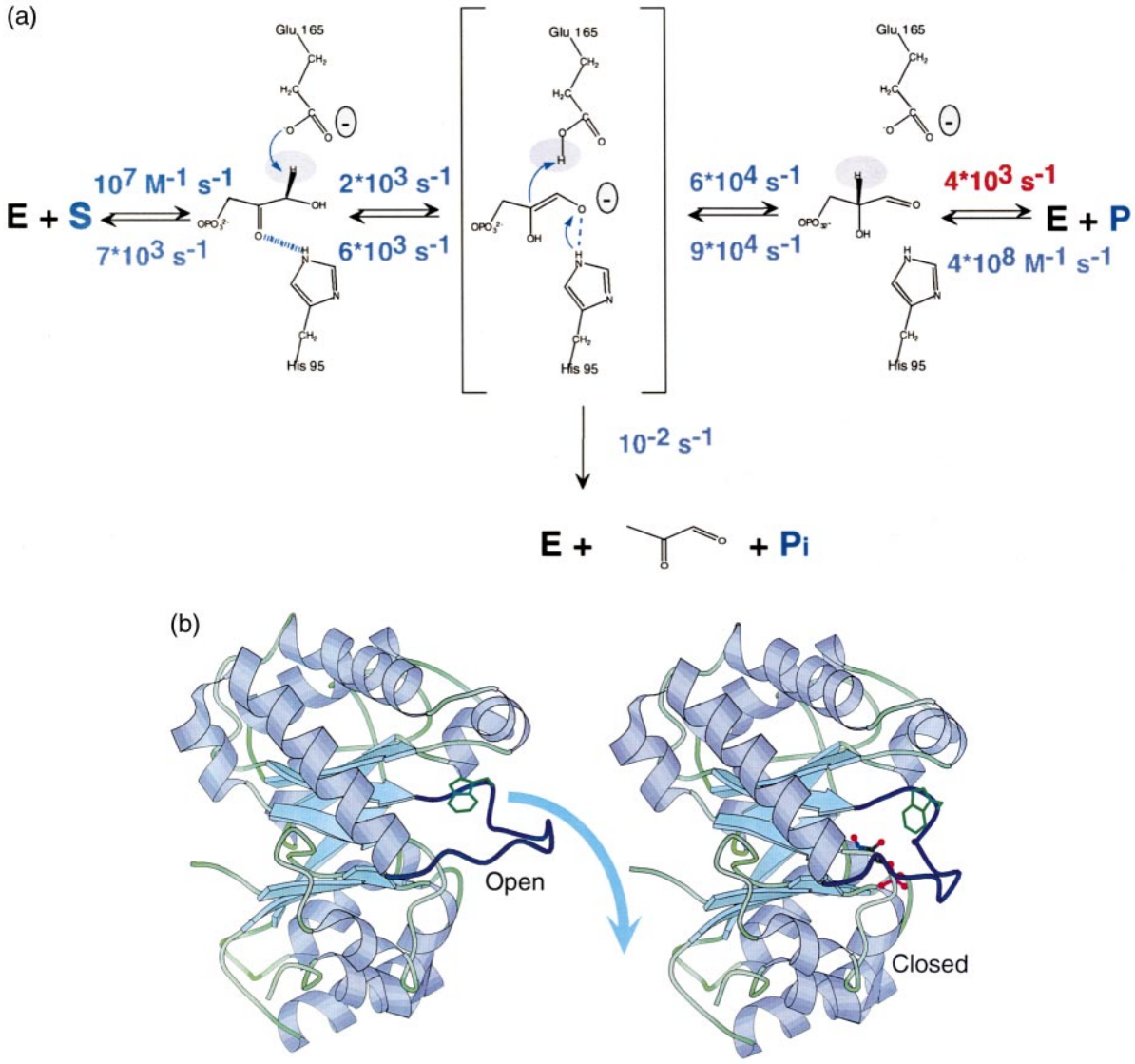

Figure 1. (a) Proposed reaction mechanism and rates constants associated with the chicken Triosephosphate isomerase as measured by Albery, Knowles and coworkers (Albery & Knowles, 1976b). Dihydroxyacetone phosphate (DHAP) and D-glyceraldehyde 3-phosphate (GAP) are made in equal amounts by aldolase; during resting physiology TIM must convert DHAP to GAP for optimal metabolic efficiency to prevent accumulation of DHAP. The rate-limiting step in this direction, shown in red, is associated with either release of the product or a slow conformational change preceding it. (b) X-ray structures indicate substantial motion during binding and release. Loop 6 moves as a rigid entity and some residues are displaced by as much as 10 Å. Yeast Triosephosphate isomerase is shown in the unligated state (PDB entry 1YPI (Lolis *et al.*, 1990)) and in the presence of a transition state analogue phosphoglycolohydroxamate (PDB entry 7TIM (Davenport *et al.*, 1991)). The N-terminal hinge tryptophan is used as a reporter in this study. Trp168 is rotated from its position in the unligated enzyme, breaking its aromatic packing interactions with N-hinge tyrosine and proline residues, to lie above the loop plane. The excursion angles for the ring deuterons are 11, 32, 39, 50 and 55°. Graphical representations were prepared with the program MOLSCRIPT (Kraulis, 1991).

facilitates binding and release while the closed conformation catalyzes the chemical reaction. The closed loop environment organizes several ionizable resides around the substrate to facilitate the core of the chemical reactions, a proton transfer between C1 and C2 methylene *via* the active site Glu165 with stabilization offered from the nearby neutral His95. The key catalytic residue, Glu165, moves in coordination with the loop. In the empty enzyme Glu165 is hydrogen bonded to Ser96 (Lolis *et al.*, 1990); upon ligand binding this hydrogen bond is broken and a 2 Å shift positions Glu165 in contact with the substrate (Davenport *et al.*, 1991; Lolis & Petsko, 1990). In the closed loop environment the low dielectric constant in the active site increases the enzyme's ability to moderate the stability of the transition state and intermediates.

While X-ray structural data indicate two strongly populated conformers, they provide no clear information about kinetic aspects. The relation between protein sequence, the rate of the loop motion and enzyme kinetics is relatively unexplored experimentally. The rate of the interconversion of the open and closed forms can be viewed as a separate issue from the relative stabilities of the open and closed forms. Although the ratios are constrained by the affinity, $(k_{off}/k_{on})(k_{open}/k_{closed}) = K_d$, a barrier for the loop motion imposed by the protein can depress both the open and closed rates and thereby determine the order of magnitude of these rate constants without affecting the stabilities or binding constants. In absence of experimental data it is conceivable that the loop opening rate could be as slow as ~100 μs, or as fast as ~0.1 ns. The purpose of this work is to clearly document the timescale of the loop opening and test the hypothesis that it is rate determining for function.

To this end, we have been developing NMR measurements to document loop motion rates. Solid state NMR is capable of providing information about motions on time scales ranging continuously from seconds to pico-seconds, while preserving details of orientation dependence, and therefore was used to study TIM loop motion (Palmer *et al.*, 1996; Spiess, 1978). Previously, deuterium NMR was used to probe the dynamics of the flexible loop in TIM, particularly the motion timescale and the ligands dependence (Williams & McDermott, 1995). Small angle motions on a nanosecond timescale were proposed and larger angle motions on the microsecond timescale were evident. A model was presented that embodied information from the crystallographic studies and the NMR studies. Putatively, the loop opens and closes on a time scale slightly faster than the enzyme turnover rate and the two predominant conformers, open and closed coordinates from crystallography, are unequally populated. Here, we show detailed temperature dependent and ligand dependent data that characterize the motion in the presence of the substrate or substrate analogues, and allow us to measure the rate constants much more accurately. Along with additional solution studies in the accompanying paper (Rozovsky *et al.*, 2001), these data allow us to demonstrate that loop motion is probably partially rate determining for the catalytic reaction.

Results

Sample conditions for NMR experiments

All experiments involved a mutant of *S. cerevisiae* TIM (Trp90Tyr Trp157Phe), in which only one tryptophan residue, Trp168, was retained and labeled with deuterons in its indole ring. This reporter tryptophan residue is conserved in all TIM sequences and is located on the N-terminal hinge of the active site flexible loop. Upon loop closure the reporter tryptophan swings by about 45° and hence is a sensitive indicator of the loop conformation and dynamics. The Trp90Tyr Trp157Phe mutant displays Michaelis-Menten kinetics close to those of the wild-type enzyme (Sampson & Knowles, 1992). The mutant enzyme structure is essentially indistinguishable from the wild-type yeast enzyme structure (Rozovsky *et al.*, 2001). Wild-type *S. cerevisae* TIM exhibits a k_{cat} value of $(8.7 \pm 0.3) \times 10^3$ s^{-1} at 30 °C (Nickbarg & Knowles, 1988) (GAP as substrate), while the (Trp90Tyr Trp157Phe) mutant k_{cat} is $(5.5 \pm 1.5) \times 10^3$ s^{-1} at 25 °C and $(3.5 \pm 1.5) \times 10^3$ s^{-1} in microcystalline samples containing PEG (Williams & McDermott, 1995). The crystalline environment does not hinder the ability of the loop to execute the catalytic motion (Alber *et al.*, 1981b; Johnson & Wolfenden, 1970; Rozovsky *et al.*, 2001). The microcrystals were grown under buffer conditions that give maximal activity and ligand binding; the TIM reaction profile is moderately dependent upon ionic strength and pH (Lambeir *et al.*, 1987). The enzyme survived long SSNMR signal acquisitions times: enzymatic assays were routinely conducted following NMR experiments. We previously confirmed that this enzyme is active in the crystalline form (Williams & McDermott, 1995) and could be competitively inhibited under the experimental conditions (i.e. microcrystalline suspension), thus ligands bind reversibly and rapidly with normal affinities. Under *in vivo* conditions, TIM is typically localized in a dense network of glycolytic enzymes in the cytoplasm and is probably not solubilized freely (Srere, 1987). Evidence for transient assemblies associated with F-actin and the cell membrane suggests that the enzyme is acting in variable cellular environments (e.g. viscosity, protein concentration and water availability) (Luby-Phelps, 2000). Therefore, it is not surprising that protein crystals can maintain full functionality; the solid, hydrated conditions, rather than monodispersed solutions, more closely resemble cellular conditions (Fulton, 1982).

When probing the catalytically related conformational change, the enzyme ligation state was varied to modulate the populations of the two forms and the sample temperature were varied in order to modify the time constant. In the temperature range from −15 to 45 °C, the PEG solution remains liquid (although viscous at low temperatures). Catalytic activity is expected to change by at least an order of magnitude over the temperature range. While TIM is fully active at 30 and 45 °C (Rentier-Delrue *et al.*, 1993), activity is down by about fivefold at 5 °C. Kinetic isotope effect studies demonstrated that the extent of tritium transfer from C1 of DHAP into C2 of GAP increased with decreasing the temperature, consistent with a picture in which protein motion rate changes much more over temperature than does the proton transfer rate (Harris *et al.*, 1998).

Deuterium solid echo line shapes: the unligated enzyme microsecond dynamics

The microsecond time regime, i.e. the same timescale as catalytic turnover, is a crucial regime for testing the relation between loop motion and function. SSNMR broadband deuterium line shapes and anisotropic T_2 values are extremely sensitive to motions on the catalytic turnover timescale. Due to the lack of free tumbling of the molecules, the resonance frequency is strongly orientation-dependent and the motion effects are strongly frequency or orientation dependent. For an aromatic C-D bond, the nuclear quadrupolar coupling strength is 167 kHz and the solid echo line shape (Spiess & Sillescu, 1981) is most sensitive to the motion rates of 10^3-10^6 s^{-1}, which give rise to pronounced alterations in line shape as compared with a static sample, and also give rise to short T_2 values. Observation of ''intermediate exchange kinetics'' by deuterium solids NMR is analogous to solution NMR chemical exchange experiments. One difference between the two methods is the usual bane of broadline spectroscopy: detection sensitivity for solid state measurements is inherently low and must be compensated by long signal acquisition times. The chief spectroscopic advantage to solid state spectroscopy is that the frequency changes are analytically related to angles of the reporter group relative to the applied magnetic field, rather than being empirically related to other environmental changes that may give rise to small chemical shift changes. Much larger frequency changes are typically involved, so that more dramatic effects on the line shapes and dephasing times are expected. The NMR experiment is relatively blind to certain perturbations such as ligand binding, and very sensitive specifically to the conformation change itself. Here, we take advantage of the sensitivity of the method to large angular hops, and the ability to focus specifically on these conformation changes rather than environmental effects, to distinguish between ligand binding kinetics and loop conformational kinetics.

The quadrupolar echo or T_2 experiment is a crucial tool in our study. Effects of motion on the line shape are most pronounced when the rate of motion is comparable to changes in resonance frequency during the hop. A variety of interesting line shapes arise from incomplete refocusing of magnetization when molecular motions ''compete'' with coherent evolution during the echo sequence (Wittebort *et al.*, 1987). The effect of motion on the powder pattern can be easily simulated using relatively few assumptions (Spiess & Sillescu, 1981).

Temperature-dependent line shapes of unligated TIM are presented (Figure 2) for temperatures from −15 to 45 °C. Spectra were collected with echo delays of 30, 100 and 140 μs; recycle delays were at least 5 times T_{1Z} as listed in Materials and Methods section. Lineshapes of well defined enzyme crystals and line shapes of precipitated enzyme were identical within signal-to-noise. The large narrow feature near zero frequency, due to residual liquid ^2H_2O, is deleted. The powder line shapes are largely static-like; they do not reflect substantial narrowing of the quadrupolar coupling constant nor alterations in line shape relative to the typical values for an aromatic ring, i.e. ω_Q, the quadrupolar coupling constant $\cong 2\pi \times 167$ kHz corresponding to a powder width of 250 kHz. Furthermore, the line shapes are fairly similar whether measured at 10, 30 and 45 °C. The line shapes are scaled at longer delays in what appears to be an exponential spin dephasing (T_2) decay of unknown origin. This decay is faster than that seen for a control where deuterium labeled tryptophans were incorporated into non-mobile sites (Williams & McDermott, 1995) and substantially faster than the crystalline deuteron-tryptophan control. Heteronuclear dipolar dephasing is not refocused in this pulse sequence and could contribute some of the effect. This decay is probably dominated by low angle motions that are faster than turnover but slower than the deuteron's Larmor frequency. Since many different processes could be responsible for this decay, no simulations are shown. At −15 °C an altered spectrum is observed: the center of the spectrum disappears altogether for interpulse refocussing times of 100 μs and longer. This spectrum is typical for deuterons undergoing low angle motions on the microsecond timescale. At this temperature, the sample is well above the freezing point, but is presumably quite viscous. We assume without direct proof that analogous motions occur for the sample at warmer temperatures at much faster rates (nanosecond timescale) and cause the spin lattice relaxation processes. Similar motions also appear to occur for ligated enzymes at low temperatures (Figure 4 left panel), although the spectra are not identical. Simulations (Figure 5(c)) illustrate the likely kinds of motions that are probably responsible for this altered line shape. Rare large angle loop excursions in the absence of the ligand (i.e. full closure) can not be excluded as a model for the underlying motion without probing the distribution of angles associated with this particular line shape. In order to detect the opening and closing motions, and determine their timescale unambiguously, we studied the loop in the presence of a ligand, as described below.

Large angle microsecond motion in the presence of a substrate analogue: loop opening rate

Elimination of phosphate from the reaction intermediate and the formation of the reactive methylglyoxal inactivate the enzyme. Therefore, measurements on the substrate itself are challenging, subject to limitations in concentrations, temperature and time duration. We have chosen instead to characterize the loop motion in the presence of the substrate analogue DL-α-glycerophosphate. The analogue's binding affinity and

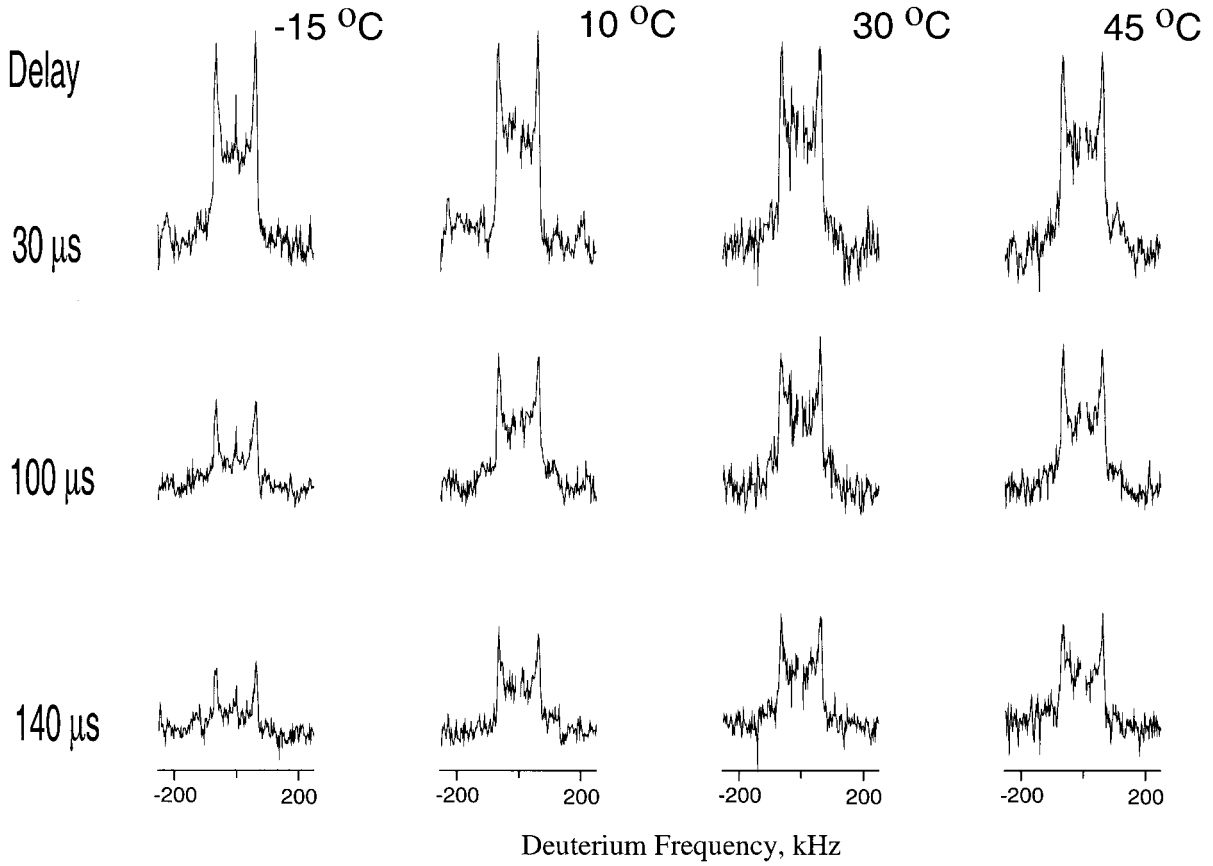

Figure 2. Deuterium SSNMR line shapes of $^2H_5$-Trp168 microcrystalline TIM in PEG (no ligand present) at temperatures from −15 to 45 °C. Interpulse echo delay time, τ, for the quadrupolar echo pulse sequence is indicated on the left (note that total relaxation time is 2 τ). Spectral line shapes are typical for a static deuteron. In each case the signal intensity decays with increasing echo delay. This decay might be due to coherent evolution under the heteronuclear (^{2}H-^{1}H) dipolar interaction, or due to T_2 processes caused by motions. Such a decay process was not observed in crystalline deuterio-tryptophan and was seen to a lesser extent for deuterons in tryptophan in other locations in TIM, or for deuterons in Trp168 in ligated samples. Spectra taken with long delay times at low temperature are characterized by anisotropic losses of magnetization: only the perpendicular features remain in the spectrum. Such an echo spectrum is indicative of low angle motions with rate constants of the order of 10^5-10^6 s^{-1}. See simulations; Figure 5(c) and Table 1.

chemical structure closely resembles that of the substrate (GAP K_m 0.055(±0.004) mM, DHAP K_m 1.4(±0.1) mM; G3P K_i 1.4(±0.3) mM, only the D-enantiomer binds appreciably (Nickbarg & Knowles, 1988)). The concentration of the substrate analogue was varied, in order to control the populations of the loop conformations, since the relative population of the two conformers greatly affects our ability to detect the motion. In addition, the temperature of the sample was maintained in a range where enzyme turnover is maximal (30-40 °C) in order to maximize the possibility of detecting functionally significant motions. Figure 3 presents echo detected line shapes of ring deuterated Trp168 in TIM in the presence of G3P, recorded at 30 °C. Dramatic losses of intensity over longer echo delays, i.e. very short dephasing (T_2) times for the deuterons are observed when the ligand concentration is adjusted so that half the enzyme active sites are occupied (presumably resulting in roughly equal population of closed and open loop conformations). The deuterium quadrupolar echo line shapes or partially ligated samples were also investigated as a function of temperature (Figure 4). The pronounced effect of ligand and temperature on T_2 is clear: dephasing is observed only if the sample temperature is at or above 30 °C and the populations of open and closed are nearly equal. Using a simplified two site physical model, motivated by the collection of X-ray studies, we estimate from simulations of these spectra that the angle of the hop must be at least 30° and that the time scale must be of the order 10^4 s^{-1} at 45 °C. This motion is attributed to the loop catalytic excursion for the following reasons: it is present only in the ligand bound samples, it is pronounced only at warmer temperatures where enzyme turnover occurs, and it is clearly associated with a large angle hop. The rate estimated is in good agreement with the rate deduced from solution-state NMR chemical exchange experiments (Rozovsky *et al.*, 2001).

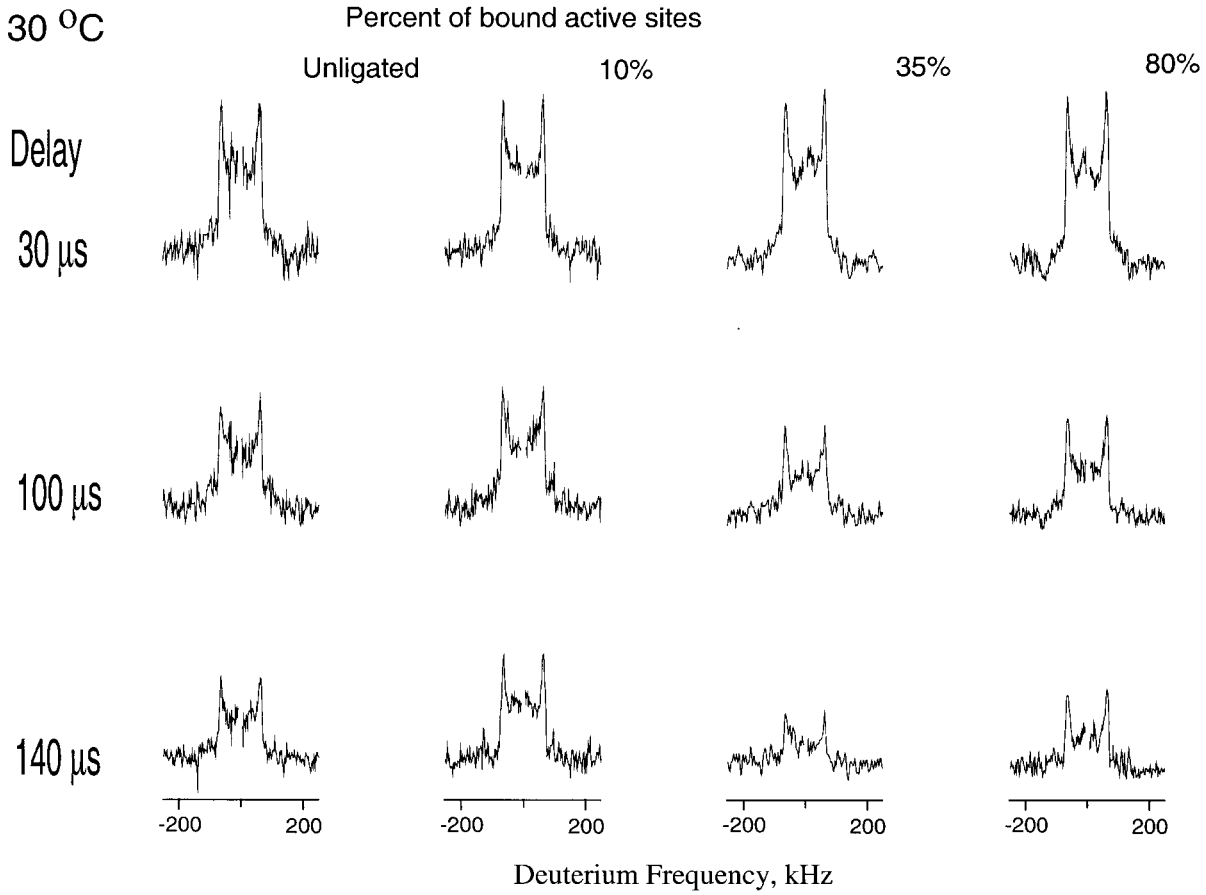

Figure 3. Deuterium SSNMR line shapes of $^2H_5$-Trp168 microcrystalline TIM in the presence of varying amounts of the substrate analogue, DL-glycerol 3-phosphate (G3P) corresponding to (from left, expressed as percentage of bound active sites): 0%, 10%, 35% and 80%. All spectra were acquired at 30 °C. Interpulse echo delay times τ are indicated to the left. When the enzyme has comparable populations of open and closed forms (e.g. the third spectrum from the left), a marked increase in the dephasing rate is seen, consistent with the suggestion of intermediate exchange kinetics: the loop opening rate, k_{open}, and the frequency difference for deuteron due to the hop, are comparable. The fact that the entire spectrum dephases indicates that the hop angle must be large, and is consistent with the suggestion that this process is the full opening and closing. The spectra cannot be explained by libration of the loop in a smaller angle. These spectra are best fit with opening times of order 3×10^3 to 10^4 s^{-1}, consistent with the rates estimated from solution NMR studies of ^{19}F label in Trp168. See simulations; Figure 5(a) and Table 1.

Line shapes recorded at 30-45 °C in the presence of subsaturating ligand concentrations provide important evidence about the timescale of loop opening. Certain kinetic features are required for any model that can explain our data: nearly equal populations of open and closed conformations, rate constants for motion of the order of 10^4 s^{-1}, and relatively large hop angles between open and closed (30 to 60 °) are needed. The data were simulated with a simple 2 or 3 site model with either one or two sequential kinetic processes, intending to represent ligand binding/release and loop opening/closing. In Figure 5 we show that the variation of T_2 values with changes in relative population of the closed and open states as well as its temperature dependence, can be reproduced, using a simple two-site model with a rate of 8000 s^{-1} at 30 °C and an angle of 40 ° for the angular excursion. The angle of 40 ° is based on the averaged tryptophan deuteron angular excursion from the X-ray structures. Rates were changed to accommodate temperature changes according to approximately Arrhenius process with a barrier of 14 kCal/mol (see Table 1 for rates).

It is important to note that the rates we report represent the loop's motion k_{open} rather than k_{on} or k_{off} (Scheme 1). Some constraints on the rate constants for steps involving loop opening, loop closing, ligand on, and ligand off can be hypothesized:

$$E + S \underset{k_{off}}{\overset{k_{on}}{\rightleftharpoons}} ES_{open} \underset{k_{open}}{\overset{k_{close}}{\rightleftharpoons}} ES_{close}$$

Scheme 1

Table 1. Simulation parameters for Figure 5

Data Figure/Panel	Simulations Figure/Panel	Percentage of closed conformer assumed[a]	Temperature (°C) (Expt.)	Rate constant[b] (Sim.)	Angle (deg.) (Sim.)
3/1	5a/1	Unligated[c]	30	8×10^3	40
3/2	5a/2	10	30	8×10^3	40
3/3	5a/3	35	30	8×10^3	40
3/4	5a/4	80	30	8×10^3	40
4/2	5b/1	35	10	3×10^3	40
4/3	5b/2	35	30	8×10^3	40
4/4	5b/3	35	45	1×10^4	40
2/1	5c/1	Unligated[d]	−15	1×10^5	2
2/2	5c/2	Unligated[d]	10	5×10^5	2
2/3	5c/3	Unligated[d]	30	1×10^6	2
2/4	5c/4	Unligated[d]	45	5×10^6	2

[a] The population ratio of the open *versus* closed loop conformation was estimated as described in Material and Methods based on total enzyme and ligand present.
[b] Rate constant for the jump from the open to the closed conformation.
[c] Approximated as having 1 % closed loop conformation from active-site protection in isotopic exchange experiments (Browne & Waley, 1974).
[d] Five sites equally populated, in a linear arrangement, with hops to nearest neighbor only.

diffusion limited on kinetics would place k_{on} at 10^9-10^{10} M^{-1} s^{-1} or 10^6-10^7 s^{-1} under our experimental conditions where ligand concentrations of 0.5-10 mM and temperatures of 10-45 °C are used. The encounter complex is always the least populated of the three forms, and therefore we can place a limit on the off rate of the ligand at $k_{off} \gg k_{on}K_d \sim 10^6$ s^{-1}. This statement is also consist-

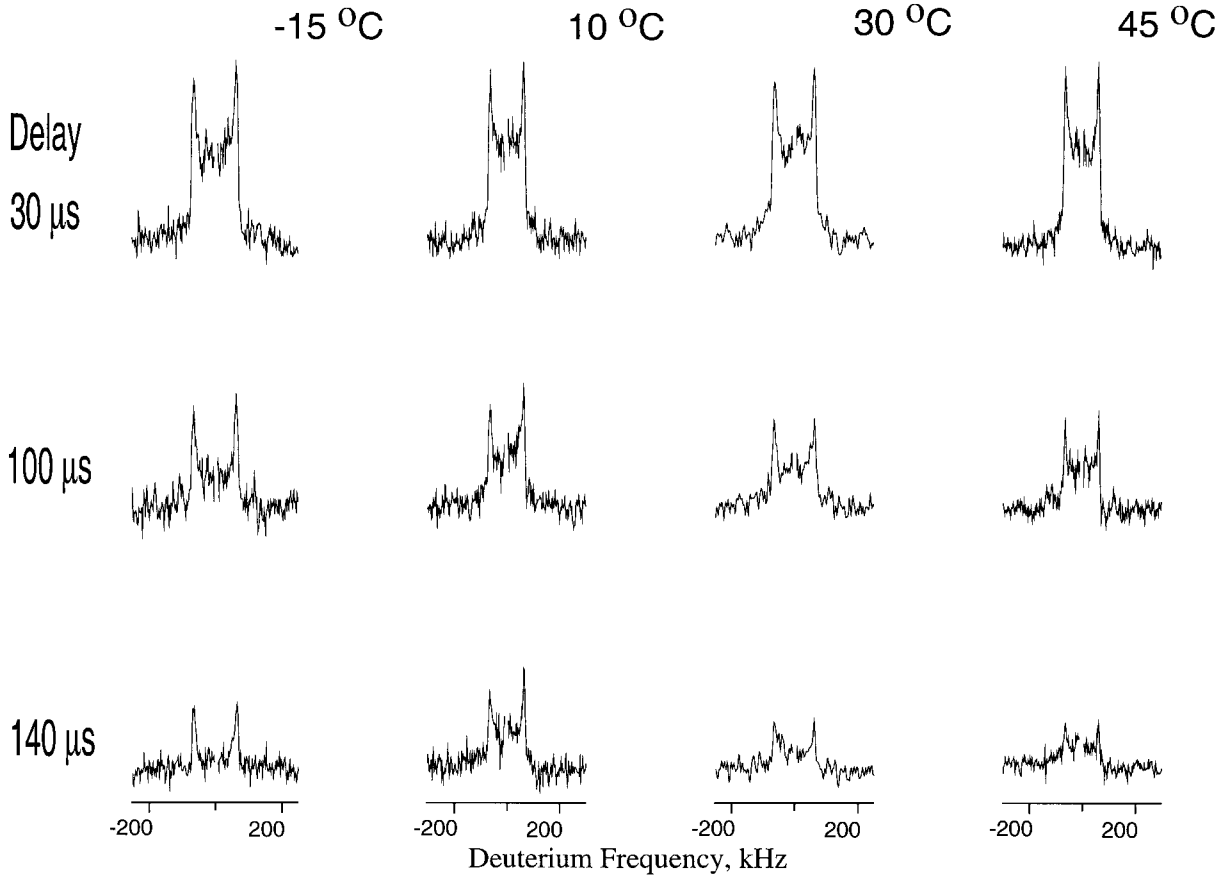

Figure 4. Temperature dependent line shapes of $^2H_5$-Trp168 microcrystalline TIM with DL-glycerol 3-phosphate with 35 % of active sites having ligand present. Deuterium quadrupolar echo spectra were collected at temperatures of −15, 10, 30 and 45 °C using delay times as indicated. Loss of magnetization with longer delay times is seen only at warmer temperatures, indicating that the loop opening motion is strongly temperature dependent. See simulations: Figure 5(b) and Table 1.

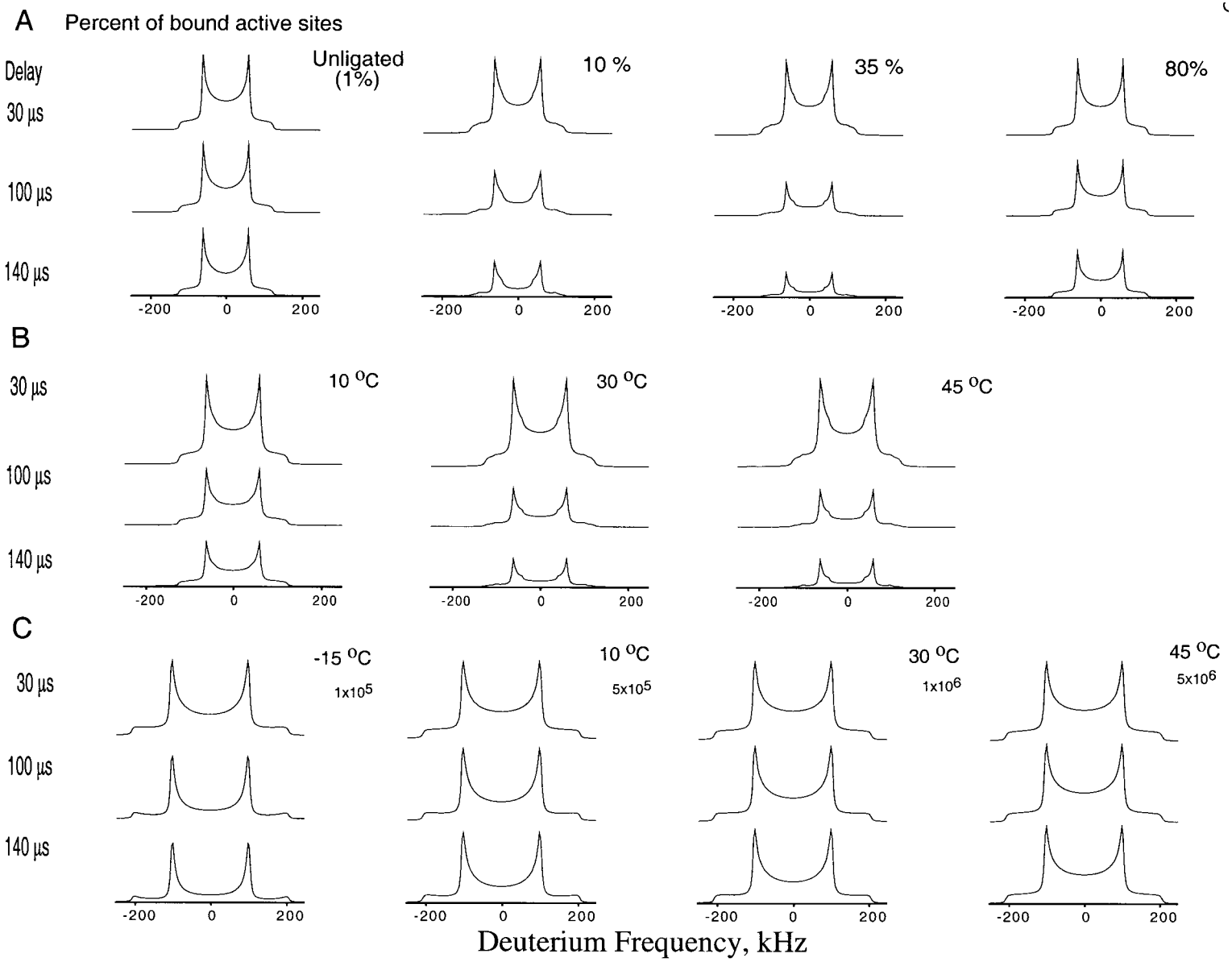

Figure 5 *(legend opposite)*

ent with the weaker affinities for the ligands on the loopless mutant form of the enzyme (Pompliano *et al*., 1990). The fact that the encounter complex is sparingly populated also allows us to know that $k_{close} \gg k_{open}$. If the protein motion is partially rate determining for overall throughput, as our NMR data argue (Rozovsky *et al*., 2001) and as was concluded on the basis of isotope studies (Albery & Knowles, 1976b), then these inequalities indicate that it must be the opening rate that is in fact rate limiting.

Dephasing and intermediate exchange behavior can only be caused by a process in which the chemical kinetic constant is of the order of the change in precession frequency; coherent evolution of the magnetization must directly compete with stochastic changes in the precession frequency. Therefore our data are not compatible with a two step process involving a slow ligand binding step with modest change in angle, followed by a rapid conformation change step with large change in angle. We cannot on the other hand rule out a picture in which the kinetics of binding and release and the loop conformation change both have microsecond rate constants and both are partially rate determining for overall throughput. Thus the data reflect that loop motion in the presence of a substrate analogue is of the order of the turnover rate, and not much faster.

It is clear that this study of one analogue compound does not address the full repertoire of the flexible loop. Our choice of ligand defines and selects conditions resembling the reaction substrate binding, onset and release. However, the flexible loop might respond to subtle changes in charges and hybridization changes during the reaction. The rate of conversion of DHAP to GAP is ten times slower than that of GAP to DHAP; nonetheless product release is rate limiting for the DHAP to GAP reaction, while proton abstraction is rate limiting for the GAP to DHAP reaction. Thus, the relation between the ligand's chemical details and the loop motion rate can be of great interest in understanding how protein dynamics are related to chemical reactivity.

Conclusions

The opening and closing motion of the active site loop 6 in TIM has a rate constant that closely matches the turnover time for catalysis. This motion causes dramatic changes in the NMR dephasing (T_2) times when the open and closed states are both substantially populated. The motion is also strongly temperature dependent. We conclude that the loop motion is likely to be partially rate determining for the chemical reaction, consistent with the observation that modest isotope effects are seen, and that apparent bimolecular association constants are depressed from their theoretical values. The strict conservation of this mobile loop 6 and a neighboring loop 7 suggest that not only is protein motion rate determining for catalysis, but that it should be rate determining for optimal function. The purpose for slow motions and long residence times in the enzyme remains to be further explored.

Materials and Methods

Materials

All reagents used were purchased from Sigma-Aldrich Co. with the exception of glycerol-3-phosphate dehydrogenase from Boehringer Mannheim Ltd. and deuterium depleted water from Cambridge Isotope Laboratories, Inc. L-[2,4,5,6,7-$^2H_5$] Tryptophan was synthesized as described by Matthews *et al*. (1977) from L-tryptophan by acid catalyzed exchange.

Figure 5. (a) Simulations of the deuterium quadrupolar line shapes as a function of ligand concentration, (Figure 3). Populations used in the simulations assume 1% closed, 10%, 35% and 80%, as estimated for the experimental data sets. The model contains two loop conformations, with an angular excursion (40°) based on average of the angles observed in the crystal structure (11, 32, 39, 50 and 55°). Additional simulations (not shown) indicate that, within our sensitivity limits, use of an average angle is an adequate model. Intensity for different samples or different simulations can not be accurately compared. The rate of loop opening is 8×10^3 s^{-1} throughout this set of simulations. The populations of the loop conformers differs through this series, thus the effective closing rate also changes. The dephasing rate T_2 is enhanced if the populations of open and closed conformers are approximately matched. Similar simulations can be achieved with a two step, three state model involving an evanescent encounter complex; agreement between simulations and data requires use of loop opening rates of order 5×10^3-10^4 s^{-1}. (b) Temperature dependent line shapes for partially ligated samples (Figure 4) were simulated assuming a two-state hopping motions with an angle of 40°, population of the closed conformer of 33%, and opening rates of 3×10^3 s^{-1} for 10 °C, 8×10^3 s^{-1} at 30 °C and 10^4 s^{-1} at 45 °C. Simulation intensities are arbitrary scaled. (c) Temperature dependent line shapes for samples at low temperatures (Figures 2 and 4, data at −15 °C) were simulated assuming a small angle (2°) hopping motions between five equally populated sites. This sort of motion might be typical for backbone librations, although this model is literally proposed to accurately define the angles involved. A hopping rate of 10^5 s^{-1} was used to simulate the data at −15 °C, a rate of 5×10^5 s^{-1} was used to simulate the data at 10°, a rate of 10^6 s^{-1} was used to simulate the data at 30 °C, and 5×10^6 s^{-1} was used for 45 °C. As the motion becomes faster than the intermediate exchange regime it no longer contributes to the anisotropic T_2, thus spectral decay due to motion is seen only at lower temperatures. Spectra in the presence of subsaturating and saturating amounts of ligand also show a similar motion.

Preparation of yeast mutant triosephosphate isomerase

The expression vector, a modified pKK223-3 containing *S. cerevisiae* (baker's yeast) Triosephosphate isomerase gene with a Trp90Tyr Trp157Phe mutation was a generous gift from Professor N. S. Sampson of SUNY, Stonybrook, and Professor J. R. Knowles of Harvard University. The enzyme was expressed in *Escherichia coli*, tryptophan auxotroph JA300 a gift from Professor D. B. Goodin of the Research Institute of Scripps Clinic.

Cells were grown in Luria broth at 37 °C, with good aeration and an ampicillin selection of 50 μg/ml. The media was substituted (at $A_{600} = 0.3$) with selected medium containing the labeled tryptophan as described previously (Williams & McDermott, 1995). After a brief equilibration period, protein expression was induced with 0.4 mM IPTG. The cell paste (2.5 g/l growth medium) following a 20-22 hour expression period was resuspended in 50 mM Tris-HCl, 150 mM NaCl, 20 mM KH_2PO_4, 1 mM EDTA, 1 mM DTT, 1 μM PMSF, pH 7.8 at 4 °C and lysed using the French press. The lysate was centrifuged at 10,000 *g* for 20 minutes to remove cell debris. Following equilibration with ammonium sulfate (45 % saturation) the precipitant was removed by centrifugation at 12,000 *g* for 20 minutes. The succeeding purification steps were conducted at room temperature. The protein solution was dialyzed extensively against 50 mM Tris-HCl, 150 mM NaCl, 1 mM EDTA, pH 7.8 at 25 °C. Nucleic acids were removed using a Q sepharose fast flow column. The enzyme solution was dialyzed against 10 mM Tris-HCl, pH 7.8 at 25 °C and purified by a Q sepharose fast flow column using a linear gradient of 0-150 mM KCl. Fractions containing the isomerase were assayed for activity. Fully active fractions were combined, dialyzed against 1.4 M ammonium sulfate, 50 mM Na_2HPO_4, pH 7.0 at 25 °C and further purified using a phenyl sepharose 6 fast flow column with a linear gradient of 1.4-0 M ammonium sulfate. Enzyme purity, as determined by 10 % SDS-PAGE gels, is higher than 95 %. Protein purity was also verified by electrospray Q-TOF mass spectrometry. All purification steps were carried in ultra pure water (Hydro services, Inc.). Protein concentration and activity were assessed and fractions were pooled and concentrated to 40 mg/ml. 1 l of culture yields above 150 mg of protein.

NMR samples

Solid state NMR samples were microcrystals formed from a solution of 80 mg/ml protein in 50 mM Tris-HCl, 50 mM NaCl, 1 mM EDTA (pH 6.8) in deuterium depleted water at 25 °C. Several exchanges of buffer were preformed to minimize ^2H_2O background. Polyethylene glycol (average molecular weight 4000) was added to the protein solution until the solution appeared cloudy; the final concentration of polyethylene glycol was 14-16 %. The solution was then clarified by addition of a minimal amount of the initial buffer and left at room temperature. For ligated samples, the ligand was cocrystallized with the enzyme. Crystals appeared within few hours in a $P2_1$ unit cell (unligated enzyme) and $P2_12_12_1$ unit cell (ligated enzyme) as determined by X-ray diffraction. Crystal sizes were roughly 0.1 mm × 0.1 mm × 0.05 mm. Crystals were packed into a 5 mm quartz tube, immersed in mother liquid. About 80 mg TIM were utilized in a typical experiment.

To estimate the percent of bound enzyme we utilize a value of 1.2 mM for the dissociation constant along with the known total concentration of enzyme and ligand (Jones & Waley, 1979):

$$K_d = \frac{1-y}{y}(L_t - S_t y)$$

where K_d is the dissociation constant, y is the fraction of bound active sites, S_t is the concentration of total binding sites, and L_t is concentration of the total ligand. Both the monoanion and dianion of D-G3P bind to the enzyme (Campbell *et al.*, 1979; Jones & Waley, 1979) (the L-enantiomer does not bind appreciably), binding is independent of pH over the range 6.5-8.5.

Activity assays

The enzymatic activity of TIM was determined by the conversion of GAP to DHAP in the presence of TIM and glycerol 3-phosphate dehydrogenase (Oesper & Meyerhof, 1950; Plaut & Knowles, 1972). Enzymes were freshly prepared in 100 mM triethanolamine-HCl (pH 7.6). The reaction mixture contained (final volume 1 ml): 100 mM triethanolamine-HCl (pH 7.6), 5 mM DL-GAP, 0.24 mM NADH, 4 units glycerol-3-phosphate dehydrogenase (0.5 mg), 10 μl of TIM solution (4 μmol, 0.04 units). Activity was measured at room temperature by monitoring the change in NADH absorbance at 340 nm. Protein concentration was measured by its absorbance at 280 nm (molar absorptivity 13250 l cm^{-1} mol^{-1}) and by Bradford assays. Enzyme stability was studied as a function of temperature, time and ligand presence. Full enzymatic activity was maintained after prolonged intervals for all of the conditions used in the experiments described. NMR samples were assayed for activity prior and following the NMR experiments.

Solid state NMR spectroscopy

NMR spectra were acquired at a field of 9.4 Tesla on a Chemagnetics CMX-400 spectrometer. Broadband deuterium NMR spectra at a Larmor frequency of 60.86 MHz were collected using a quadrupolar echo pulse sequence (90_x-τ-90_y-τ-detect) with a 90° pulse length of 1.8-2.0 μs, 500 ns digitization rate, and an accumulation of 50,000 scans. Delay between scans for the ligated enzyme was 1.2 seconds at 35 and 45 °C, three seconds at 10 °C, and five seconds at −15 °C. The delay was one second for the unligated enzyme at all temperatures except for a three seconds delay at −15 °C. The incoming excitation power was approximately 1000 W and probe quality factor Q was approximately 120. Line broadening of 2000 Hz was applied to the time domain data.

NMR simulations

Simulations of the quadrupolar echo line shape were performed using Turbopowder program (Wittebort *et al.*, 1987). The program utilizes an N-site model as described by Wittebort and Szabo (1978). Based on the superimposition backbone atoms of the yeast TIM structures (unligated TIM PDB entry 1YPI (Lolis *et al.*, 1990) and in the presence of a transition state analogue phosphoglycolohydroxamic acid PDB entry 7TIM (Davenport *et al.*, 1991)) the angular changes for the deuterons are 11, 32, 39, 50 and 55°. An average angle of 40° was used for the simulations; simulations involving inhomogeneous sums for all five angles were not substantially different from those involving a single, average value within our signal-

to-noise ratio. No finite pulse correction was applied to the line shape simulations; such a correction would reduce the shoulders of the spectrum by approximately 40% but would not substantially affect the center and horns of the spectrum. Supplemental data are located at http://www.chem.columbia.edu/~mcdhome/

Acknowledgments

The authors thank Dr Jim Frye from Varian, Inc., for valuable advice regarding broadband deuterium NMR experiments, Dr Edward O'Connor and Dr John Williams for helpful discussions and Dr Greg Petsko, of Brandeis University, for stimulating conversations regarding the TIM mechanism. This work was supported by National Institutes of Health grant GM49964.

References

Alber, T., Banner, D. W., Bloomer, A. C., Petsko, G. A., Phillips, D., Rivers, P. S. & Wilson, I. A. (1981a). On the three-dimensional structure and catalytic mechanism of triose phosphate isomerase. *Philos. Trans. R. Soc. London, ser. B,* **293**, 159-171.

Alber, T., Hartman, F. C., Johnson, R. M., Petsko, G. A. & Tsernoglou, D. (1981b). Crystallization of yeast triosephosphate isomerase from polyethylene glycol. *J. Biol. Chem.* **256**, 1356-1361.

Alber, T., Gilbert, W. A., Ponzi, D. R. & Petsko, G. A. (1983). The role of mobility in the substrate binding and catalytic machinery of enzymes. In *Mobility and Function in Proteins and Nucleic Acids* (Porter, R., O'Connor, M. & Whelan, J., eds), pp. 4-24, Ciba Foundation Symposium 93, Pitman, London.

Albery, W. J. & Knowles, J. R. (1976a). Evolution of enzyme function and the development of catalytic efficiency. *Biochemistry,* **15**, 5631-5640.

Albery, W. J. & Knowles, J. R. (1976b). Free-energy profile of the reaction catalyzed by triosephosphate isomerase. *Biochemistry,* **15**, 5627-5631.

Browne, C. A. & Waley, S. G. (1974). Studies of triosephosphate isomerase by hydrogen exchange. *Biochem. J.* **141**, 753-760.

Campbell, I. D., Jones, R. B., Kiener, P. A. & Waley, S. G. (1979). Enzyme-substrate and enzyme-inhibitor complexes of triose phosphate isomerase studied by 31P nuclear magnetic resonance. *Biochem. J.* **179**, 607-621.

Davenport, R. C., Bash, P. A., Seaton, B. A., Karplus, M., Petsko, G. A. & Ringe, D. (1991). Structure of the triosephosphate isomerase-phosphoglycolohydroxamate complex: an analogue of the intermediate on the reaction pathway. *Biochemistry,* **30**, 5821-5826.

Fulton, A. B. (1982). How crowded is the cytoplasm? *Cell,* **30**, 345-247.

Harris, T. K., Cole, R. N., Comer, F. I. & Mildvan, A. S. (1998). Proton transfer in the mechanism of triosephosphate isomerase. *Biochemistry,* **37**, 16828-16838.

Johnson, L. N. & Wolfenden, R. (1970). Change in absorption spectrum and crystal structure of triose phosphate isomerase brought about by 2-phosphoglycollate, a potential transition state analogue. *J. Mol. Biol.* **47**, 93-100.

Jones, R. B. & Waley, S. G. (1979). Spectrophotometric studies on the interaction between triose phosphate isomerase and inhibitors. *Biochem. J.* **179**, 623-630.

Joseph, D., Petsko, G. A. & Karplus, M. (1990). Anatomy of a conformational change: hinged ''lid'' motion of the triosephosphate isomerase loop. *Science,* **249**, 1425-1428.

Knowles, J. R. (1991). To build an enzyme. *Philos. Trans. R. Soc. London, ser. B,* **332**, 115-121.

Komives, E. A., Chang, L. C., Lolis, E., Tilton, R. F., Petsko, G. A. & Knowles, J. R. (1991). Electrophilic catalysis in triosephosphate isomerase: the role of histidine-95. *Biochemistry,* **30**, 3011-3019.

Komives, E. A., Lougheed, J. C., Liu, K., Sugio, S., Zhang, Z., Petsko, G. A. & Ringe, D. (1995). The structural basis for pseudoreversion of the E165D lesion by the secondary S96P mutation in triosephosphate isomerase depends on the positions of active site water molecules. *Biochemistry,* **34**, 13612-13621.

Kraulis, P. J. (1991). MOLSCRIPT: a program to produce both detailed and schematic plots of protein structures. *J. Appl. Crystallog.* **24**, 946-950.

Lambeir, A. M., Opperdoes, F. R. & Wierenga, R. K. (1987). Kinetic-properties of triose-phosphate isomerase from trypanosoma-brucei-brucei: a comparison with the rabbit muscle and yeast enzymes. *Eur. J. Biochem.* **168**, 69-74.

Lodi, P. J. & Knowles, J. R. (1991). Neutral imidazole is the electrophile in the reaction catalyzed by triosephosphate isomerase: structural origins and catalytic implications. *Biochemistry,* **30**, 6948-6956.

Lolis, E. & Petsko, G. A. (1990). Crystallographic analysis of the complex between triosephosphate isomerase and 2-phosphoglycolate at 2.5 Å resolution: implications for catalysis. *Biochemistry,* **29**, 6619-6625.

Lolis, E., Alber, T., Davenport, R. C., Rose, D., Hartman, F. C. & Petsko, G. A. (1990). Structure of yeast triosephosphate isomerase at 1.9 Å resolution. *Biochemistry,* **29**, 6609-6618.

Luby-Phelps, K. (2000). Cytoarchitecture and physical properties of cytoplasm: volume, viscosity, diffusion, intracellular surface area. *Inter. Rev. Cyt.* **192**, 189-221.

Maister, S. G., Pett, C. P., Albery, W. J. & Knowles, J. R. (1976). Energetics of triosephosphate isomerase: the appearance of solvent tritium in substrate dihydroxyacetone phosphate and in product. *Biochemistry,* **15**, 5607-5612.

Matthews, H. R., Matthews, K. M. & Opella, S. J. (1977). Selectively deuterated amino acids analogues synthesis, incorporation into proteins and NMR properties. *Biochim. Biophysic. Acta,* **497**, 1-13.

Nickbarg, E. B. & Knowles, J. R. (1988). Triosephosphate isomerase: energetics of the reaction catalyzed by the yeast enzyme expressed in *Escherichia coli*. *Biochemistry,* **27**, 5939-5947.

Oesper, P. & Meyerhof, O. (1950). The determination of triose phosphate isomerase. *Arch. Biochem. Biophys.* **27**, 223-233.

Palmer, A. G., Williams, J. C. & McDermott, A. (1996). Nuclear magnetic resonance studies of biopolymer dynamics. *J. Phys. Chem.* **100**, 13293-13310.

Phillips, D. C., Rivers, P. S., Sternberg, M. J. E., Thornton, J. M. & Wilson, I. A. (1976). Structure and function of consecutive glycolytic enzymes. *Biochem. Soc. Trans.* **5**, 642-646.

Plaut, B. & Knowles, J. R. (1972). pH-dependence of the triose phosphate isomerase reaction. *Biochem. J.* **129**, 311-320.

Pompliano, D. L., Peyman, A. & Knowles, J. R. (1990). Stabilization of a reaction intermediate as a catalytic device: definition of the functional role of the flexible loop in triosephosphate isomerase. *Biochemistry,* **29**, 3186-3194.

Rentier-Delrue, F., Mande, S. C., Moyens, S., Terpstra, P., Mainfroid, V. & Goraj, K. M. L. *et al*. (1993). Cloning and overexpression of triosephosphate isomerase genes from phychrophilic and thermophilic bacteria. *J. Mol. Biol.* **229**, 85-93.

Richard, J. P. (1991). Kinetic parameters for the elimination reaction catalyzed by triosephosphate isomerase and an estimation of the reaction's physiological significance. *Biochemistry,* **30**, 4581-4585.

Rieder, S. V. & Rose, I. A. (1959). The mechanism of the triosephosphate phosphate reaction. *J. Biol. Chem.* **234**, 1007-1010.

Rose, I. A. (1962). Mechanisms of C-H bond cleavage in aldolase and isomerase reactions. *Brookhaven Symp. Biol.* **15**, 293-309.

Rozovsky, S., Jogl, G., Tong, L. & McDermott, A. E. (2001). Solution-state NMR inoestigations of triosephosphate isomerase active site loop motion: ligand release in relation to active site loop dynamics. *J. Mol. Biol.* **309**, 839-849.

Sampson, N. S. & Knowles, J. R. (1992). Segmental movement: definition of the structural requirements for loop closure in catalysis by triosephosphate isomerase. *Biochemistry,* **31**, 8482-8487.

Spiess, H. W. (1978). Rotations of molecules and nuclear spin relaxation. *NMR: Basic Princ. Prog.* **15**, 55-214.

Spiess, H. W. & Sillescu, H. (1981). Solid echoes in the slow motion region. *J. Magn. Reson.* **42**, 381-389.

Srere, P. A. (1987). Complexes of sequential metabolic enzymes. *Ann. Rev. Biochem.* **56**, 89-124.

Wierenga, R. K., Noble, M. E., Postma, J. P., Groendijk, H., Kalk, K. H., Hol, W. G. & Opperdoes, F. R. (1991). The crystal structure of the ''open'' and the ''closed'' conformation of the flexible loop of trypanosomal triosephosphate isomerase. *Proteins: Struct. Funct. Genet.* **10**, 33-49.

Williams, J. C. & McDermott, A. E. (1995). Dynamics of the flexible loop of triosephosphate isomerase: the loop motion is not ligand gated. *Biochemistry,* **34**, 8309-8319.

Wittebort, R. J. & Szabo, A. (1978). Theory of NMR relaxation in macromolecules: restricted diffusion and jump models for multiple internal rotations in amino acids side-chains. *J. Chem. Phys.* **69**, 1722-1736.

Wittebort, R. J., Olejeniczak, E. T. & Griffin, R. G. (1987). Analysis of deuterium nuclear magnetic resonance line shapes in anisotropic media. *J. Chem. Phys.* **86**, 5411-5420.

Edited by P. E. Wright

(Received 27 October 2000; received in revised form 28 March 2001; accepted 2 April 2001)